Development of VCSELs for Atomic Clock Applications

Dietmar Wahl, Daniel Steffen Setz, and Ahmed Al-Samaneh

This article describes the process of transferring an 850 nm VCSEL structure to devices emitting at 895 nm, a wavelength required for cesium-based atomic clocks. We discuss all the effects to be considered and present photoluminescence measurements of the modified quantum well structure. In addition, the influence of δ-doping in distributed Bragg reflectors on VCSEL characteristics, namely threshold current, maximum output power, and differential quantum efficiency, is investigated.

1. Introduction

The miniaturization of classical atomic clocks is limited by the size of the microwave resonator. The only way to achieve a further volume reduction is to move to a clock concept which does not rely on such a resonator. Concepts of miniaturized atomic clocks (MACs) based on the effect of *coherent population trapping* (CPT) have been discussed since 1993 [1] and demonstrated in the last few years [2]. The effect of CPT is based on the quantum mechanical phenomenon that the population probability of the highest energy level in a three-level system can be drastically reduced if the atom is illuminated by two coherent light sources whose emission wavelengths match the transition energies between the two lower states and the upper state [3]. A gas of atoms in this condition shows reduced absorption or increased transparency, therefore this phenomenon is also called *electromagnetically induced transparency*. Normally two separate lasers are used to achieve this effect. If the energy levels of the two lower states are very close, it is also possible to produce light with the two required wavelengths by modulating a single laser source with a frequency that corresponds to half of the energy gap between the two lower states. One then makes use of the modulation sidebands.

Vertical-cavity surface-emitting lasers (VCSELs) are of great interest for this application because of various reasons. The most important advantages of VCSELs for MAC applications are the excellent modulation capability (up to more than 10 GHz), high temperature stability, and the small power consumption of just a few mW. For a MAC, the same gases as in classical atomic clocks, namely Rb and Cs, are favored, requiring laser wavelengths of 780 nm (Rb D_2 transition), 795 nm (Rb D_1), 852 nm (Cs D_2), or 895 nm (Cs D_1) [4]. In what follows we will focus on Cs-based clocks. Because of a higher figure of merit, the D_1 transition is preferred [5]. VCSELs emitting at the required wavelength of 895 nm can be easily produced with the well-known InGaAs/AlGaAs material system. An application in MACs presumes polarization-stable laser sources which can also be fulfilled by VCSELs. Devices with monolithic surface gratings for polarization control have been recently demonstrated and investigated [6].

2. Transferring a VCSEL Design From 850 to 895 nm

In order to fabricate VCSELs with a wavelength of 895 nm for MAC applications, there are some subjects to consider if, like in our case, a design for a different wavelength already exists.

Firstly the quantum well structure in the active region of the laser has to be adjusted in a way that the energy level of the ground state of the quantum well fits to the new emission wavelength. Because the desired wavelength is larger than the wavelength corresponding to the bandgap energy of GaAs, the AlGaAs material system used so far has to be expanded by introducing indium into the quantum wells in order to achieve a reduction of the bandgap energy. In contrast to the nearly lattice-matched growth of AlGaAs, InGaAs grown on GaAs is compressively strained. This has to be considered for calculations as well as the effect of bandgap renormalization which is a many-body effect and depends on the carrier density. Finally also the influence of the band offset of the InGaAs/AlGaAs junction has to be regarded. Calculations of the quantum well energy levels for a well width of 8 nm and a barrier material of $Al_{0.27}Ga_{0.73}As$ result in a required indium content of 6 % for achieving the desired emission wavelength of 895 nm.

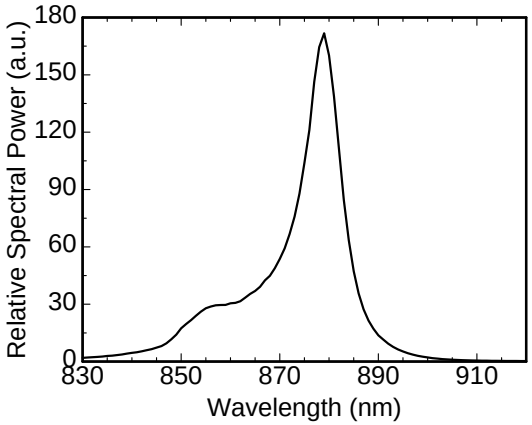

Fig. 1: Photoluminescence spectrum of an $In_{0.06}Ga_{0.94}As/Al_{0.27}Ga_{0.73}As$ quantum well, taken at room temperature.

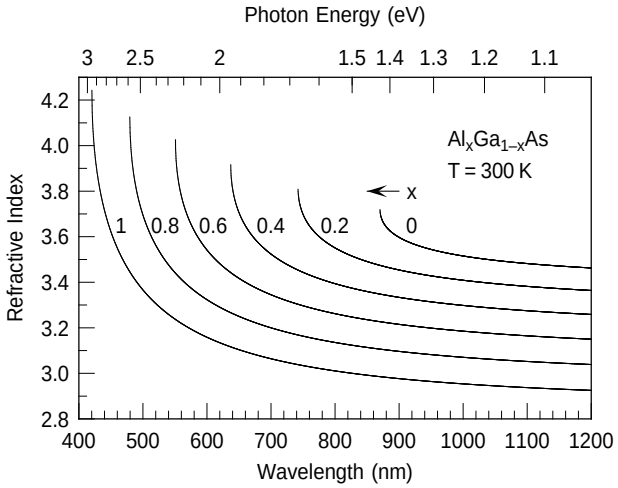

Fig. 2: Refractive index of $Al_xGa_{1-x}As$ in dependence of the aluminum concentration x and the wavelength.

In order to check the emission wavelength of the designed quantum well structure, a sample with several $In_{0.06}Ga_{0.94}As/Al_{0.27}Ga_{0.73}As$ quantum wells was grown by molecular beam epitaxy (MBE). Figure 1 depicts the photoluminescence (PL) spectrum of this sample, obtained at room temperature. The intensity maximum is found at a wavelength of 879 nm. At first glance this seems to be too small for the target wavelength of 895 nm. However, one has to consider that the carrier density in a laser is some orders of magnitude larger than that in PL experiments. For typical carrier densities in a lasing VCSEL, the effect of bandgap renormalization red-shifts the emission wavelength by about 15 nm. So, under lasing conditions, a quantum well structure like in this sample leads to an emission wavelength in the desired wavelength range.

The second step of redesigning the device is the adjustment of the layer thicknesses so that, for instance, one period of a Bragg mirror remains one half of the target wavelength in the material. The thicknesses of all layers have to be increased because of two effects: the longer wavelength itself and the reduced refractive index (Fig. 2).

Figure 3 depicts the light–current–voltage characteristics of a fabricated VCSEL with an active diameter of 4.4 µm after the above-mentioned adjustments have been made. Its threshold current is lower than 0.5 mA. The spectrum of this VCSEL operating in continuous-wave mode at a current of 2.38 mA is illustrated in Fig. 4. The fundamental transverse mode is lasing at 894.6 nm, which is the required emission wavelength for Cs-based MACs. A higher-order transverse mode is located on the short-wavelengths side with a side-mode suppression ratio of more than 25 dB, which is high enough for the present application.

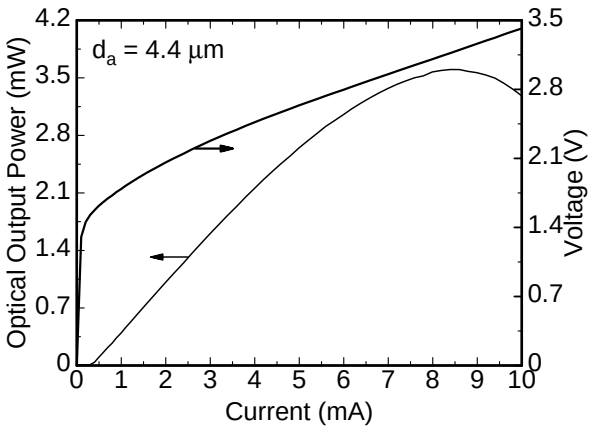

Fig. 3: Operation characteristics of an 895 nm VCSEL with 4.4 µm active diameter.

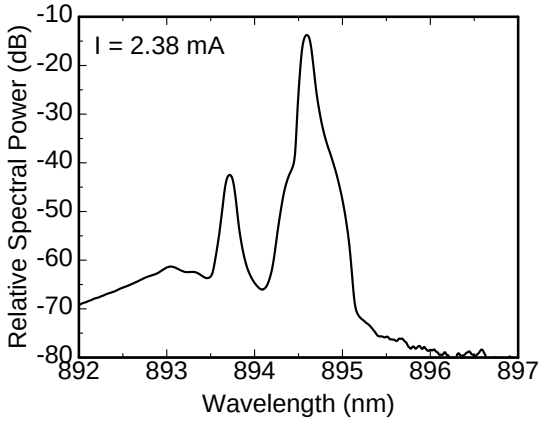

Fig. 4: Spectrum of the VCSEL from Fig. 3 at 2.38 mA current and $T = 300$ K ambient temperature.

3. Investigations Into δ-Doping of Distributed Bragg Reflectors

3.1 Composition of DBRs in VCSELs

Distributed Bragg reflectors (DBRs) of VCSELs contain several periods of layers, each of them having a thickness of half the material wavelength of the laser emission. In each period the aluminum composition of AlGaAs layers changes between low and high values in order to create a refractive index profile which gives a high reflectivity. Figure 5 shows such an aluminum composition profile of a Bragg mirror for an 895 nm VCSEL and the position of the δ-doping. The δ-doping is incorporated into the rising slope of the energy profile of the DBR (referring to the flow direction of the corresponding carriers) to reduce the ohmic resistance of the mirror.

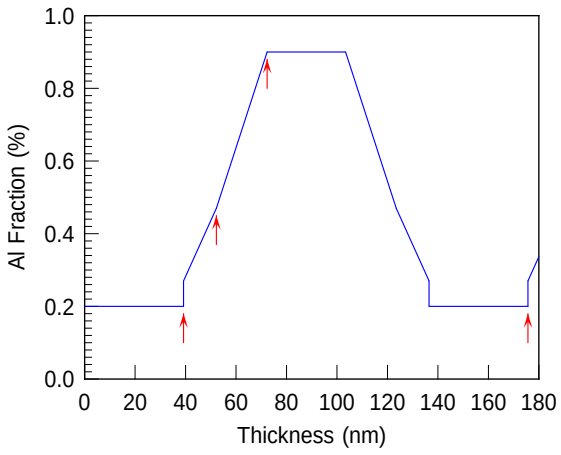

Fig. 5: Al composition profile of a Bragg mirror period. The vertical arrows indicate the positions of δ-doping.

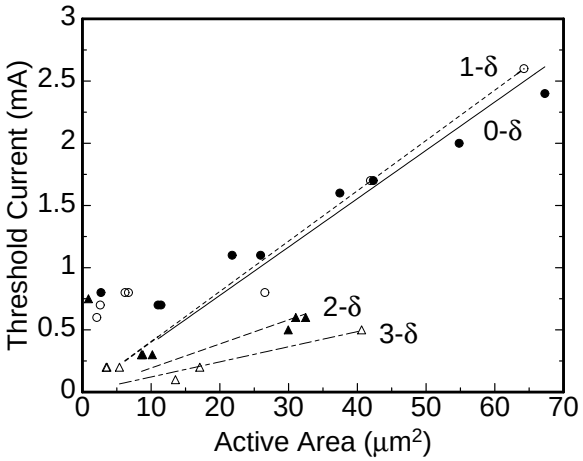

Fig. 6: Threshold current over the active area for the four investigated samples.

3.2 Influence on the electrical and optical properties

In order to investigate the influence of δ-doping in the DBRs on the laser properties, samples with different levels of δ-doping were grown by molecular beam epitaxy. All parameters except the doping level of the δ-doping were held constant within the investigated sample series. Samples without δ-doping and doping levels of 1×, 2×, and 3× a reference level of $1 \cdot 10^{12}\,\mathrm{cm}^{-2}$ for n-type material and $2 \cdot 10^{12}\,\mathrm{cm}^{-2}$ for p-type material were produced. Processing into oxide-confined VCSELs after epitaxial growth involves mesa etching, oxidation of the current aperture, and metallization of the electric contacts. The VCSELs were tested "on-wafer" without separation, i.e., all measurements were performed by contacting the lasers using contact needles. The examined parameters are threshold current, maximum output power, and differential quantum efficiency.

Concerning the threshold current in dependence of the active area, the samples without and with normal δ-doping concentrations show nearly the same behavior, as can be noticed from Fig. 6. With 2-δ concentration, the threshold current decreases drastically, and even a further reduction was achieved by tripling the doping level. The maximum output powers plotted in Fig. 7 versus the active diameter show only small deviations with variations in the δ-doping level. Highest output powers are achieved with double δ-doping concentration. No δ-doping and normal δ-doping devices show nearly the same lowest output power characteristics. The behavior of 3-δ VCSELs having a lower maximum output power than the optimum case might be due to increased optical losses induced by the higher doping concentration. As for the threshold current and output power, the differential quantum efficiencies of 0-δ and 1-δ samples show no big difference. As noticable in Fig. 8, they are nearly constant at a value of 37 % for a wide range of active diameters. Double-δ VCSELs have the highest efficiencies of more than 40 %, increasing with active diameter. This behavior is even enhanced in the 3-δ sample, as indicated by the higher slope in Fig. 8. Depending on the active size, the efficiency can be smaller than that of the low-doped samples or exceed 40 %.

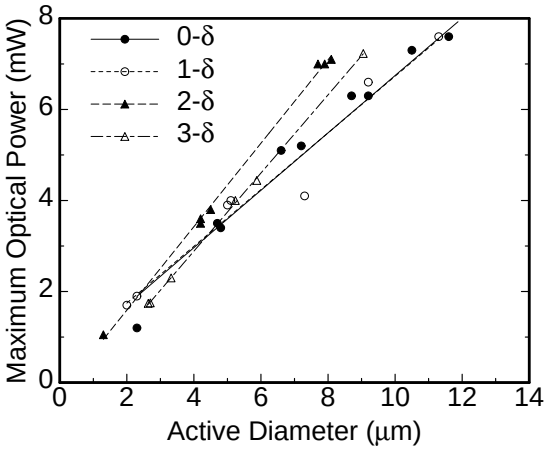

Fig. 7: Maximum VCSEL output power over the active diameter for all samples.

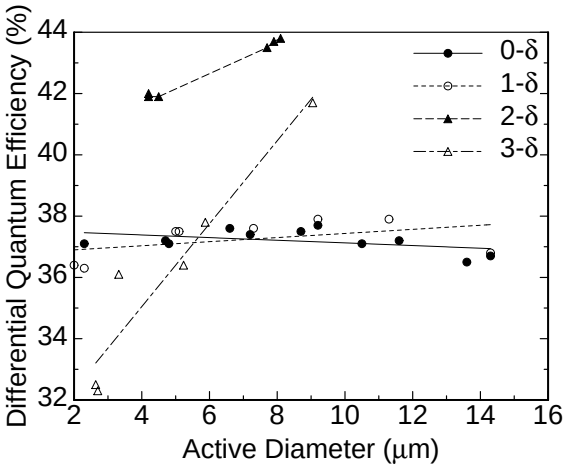

Fig. 8: Differential quantum efficiencies of the VCSELs from Fig. 7.

4. Conclusion

The transfer of an 850 nm VCSEL design to a wavelength of 895 nm has been achieved by introducing indium into the quantum wells to adjust the emission wavelength and by scaling all layer thicknesses to the new wavelength. Despite the small amount of indium in the active region, VCSELs for MAC applications can be produced within the well-known and well-controllable AlGaAs material system. First generation 895 nm wavelength VCSELs were presented to show the feasibility of this approach.

The investigation of the effect of δ-doping in the DBRs reveals that samples with no δ-doping and samples doped with the reference value show nearly no difference in threshold current, maximum output power, and differential quantum efficiency. If the level of δ-doping is doubled, the threshold current strongly decreases and higher maximum output powers as well as higher differential quantum efficiencies are achieved. For tripled δ-doping concentration, the results show inconsistent behavior. Although the threshold current is further decreased, the maximum output powers fall below those of the double-doped sample. A large variation of differential quantum efficiency with active diameter is obtained. In particular, the efficiency is drastically reduced for VCSELs with small active diameter. It seems that a doubling of the δ-doping concentration in the Bragg mirrors brings advantages to the VCSEL characteristics, however, increasing the concentration beyond this value appears not to be beneficial for future optimizations of VCSELs. Since the investigated 895 nm samples are conceptually identical to conventional 850 nm VCSELs, the results can also be transferred to other wavelengths.

Acknowledgments

We sincerely thank Fernando Rinaldi for his help with the quantum mechanical calculations and general advice as well as Susanne Menzel and Rudolf Rösch for their help with processing and metallization of the samples.

References

[1] N. Cyr, M. Têtu, and M. Breton, "All-optical microwave frequency standard: a proposal", *IEEE Transactions on Instrumentation and Measurement*, vol. 42, no. 2, pp. 640–649, 1993.

[2] S. Knappe, V. Shah, P.D.D. Schwindt, L. Hollberg, and J. Kitching, "A microfabricated atomic clock", *Appl. Phys. Lett.*, vol. 85, no. 9, pp. 1460–1462, 2004.

[3] E. Arimondo and G. Orriols, "Nonabsorbing atomic coherences by coherent two-photon transitions in a three-level optical pumping", *Lettere al nuovo cimento*, vol. 17, no. 10, pp. 333–338, 1976.

[4] D.K. Serkland, G.M. Peake, K.M. Geib, R. Lutwak, R.M. Garvey, M. Varghese, and M. Mescher, "VCSELs for atomic clocks", in Vertical-Cavity Surface-Emitting Lasers X, C. Lei, K.D. Choquette (Eds.), Proc. SPIE 6132, pp. 613208-1–11, 2006.

[5] R. Lutwak, D. Emmons, T. English, W. Riley, A. Duwel, M. Varghese, D.K. Serkland, and G.M. Peake, "The chip-scale atomic clock – recent development progress", in Proc. *35th Annual Precise Time and Time Interval (PTTI) Meeting*, pp. 467–478. San Diego, CA, USA, Dec. 2003.

[6] R. Michalzik, J.M. Ostermann, and P. Debernardi, "Polarization-stable monolithic VCSELs" (invited), in Vertical-Cavity Surface-Emitting Lasers XII, C. Lei, J.K. Guenter (Eds.), Proc. SPIE 6908, pp. 69080A-1–16, 2008